

The potential energy curve and Langmuir isotherm of hydrogen adsorption by a truncated carbon sphere

Shigeru Ishikawa¹ · Tokio Yamabe²

Received: 12 December 2014 / Accepted: 15 March 2015 / Published online: 24 March 2015
© Springer-Verlag Berlin Heidelberg 2015

Abstract The potential energy curve for the adsorption of a hydrogen molecule by a truncated hollow sphere consisting of carbon atoms was evaluated by using the Lennard–Jones function for the pair interaction between a carbon atom and a hydrogen molecule. The sphere surface was regarded as a continuum with a uniform density identical to that of a graphite layer. The lower limit of the potential was found to be -200 meV when the sphere had a radius of 3.4 Å and no opening. By increasing the radius of the opening to 2.9 Å, the energy barrier for an incoming molecule disappeared and the lower limit increased to -150 meV, which is three times as deep as that observed for a graphite surface. The Langmuir isotherm for the truncated sphere of this size was evaluated based on the eigenvalues of the potential curve. We found that the pressure yielding a half occupancy was <50 bar at a temperature below 250 K. This indicates that a carbon pore with this shape and size can store a hydrogen molecule under mild conditions.

1 Introduction

A secure hydrogen storage system with small size and light weight is indispensable for transportation, stationary, and portable applications of fuel cells and also for hydrogen delivery and refueling facilities. Currently, fuel cell

vehicles need 4 – 10 kg of hydrogen to travel a distance of approximately 480 km and require the storage of this amount in the fuel tank with a volumetric density of 40 – 70 g/L and a gravimetric density of 5.5 – 7.5 wt% [1].

The storage systems currently under development or investigation can be classified into two categories: physical storage by compression or liquefaction and materials-based storage by physisorption or chemisorption. Currently, high-pressure compressed tanks have achieved storage densities of 17 – 25 g/L and 2.8 – 4.4 wt% under pressures between 350 and 700 bar and have been adopted in prototype or commercial vehicles [1]. However, to manage hydrogen safely and to reduce the energy for compression, hydrogen should be stored at lower pressures and this restriction necessitates the development of materials-based storage. At present, the main problems involving materials-based storage are the increase of storage density without cryogenic conditions for physisorption materials and control of the kinetics during the adsorption/desorption process for chemisorption materials.

Turning our interest to physisorption materials, hydrogen gas is usually adsorbed under cryogenic conditions because the adsorption force acting on a hydrogen molecule is very weak owing to its small polarizability. To operate hydrogen storage near-ambient temperature and moderate pressures, the substrates need to increase the adsorption energy to 150 meV per hydrogen molecule [2]. Among the physisorption materials, carbon materials, such as activated carbons and carbon nanotubes, have been extensively studied because they adopt various porous structures with high stability and low weight. However, their hydrogen adsorption energies are about 50 meV [3, 4], and their storage densities are less than those of the high-pressure tanks even under cryogenic conditions [5]. Conversely, theoretical studies predict that carbon

✉ Shigeru Ishikawa
sisikawa@keyaki.cc.u-tokai.ac.jp

¹ Department of Chemistry, Faculty of Science, Tokai University, 4-1-1 Kitakaname, Hiratsuka 259-1292, Japan

² Nagasaki Institute of Applied Science, 536 Aba-machi, Nagasaki 851-0193, Japan

materials can increase their adsorption energies to 100 meV or higher and achieve a large storage density if their pore size is around 7 Å [6–8]. This prediction is consistent with the experimental observation that the hydrogen storage in carbon materials increases with a decrease of the pore size to 7 Å or below [9]. A lot of research into the optimal pore size of the carbon nanotubes and carbon slits has been performed using various methods [10–21].

Previously, we evaluated the hydrogen adsorption energies of nanocarbons with different shapes and sizes by using the Lennard–Jones potential function and determined the optimum nanostructure for storage [21]. The shapes of the nanocarbons we examined were a pair of disks, a cylinder with open ends, and a truncated sphere. Situating a hydrogen molecule in each cavity, we calculated the adsorption potential curve with various cavity sizes and obtained the lower limit of the potential depth and the optimum cavity width: –94 meV for a pair of infinite disks with a separation of 5.78 Å, –158 meV for an infinite cylinder with a diameter of 6.28 Å, and –203 meV for a closed sphere with a diameter of 6.74 Å. The potential depth of the pair of finite disks approached the lower limit when the disk diameter was larger than three times the optimum separation and that of the finite cylinder approached the limit when the cylinder length was greater than double the optimum diameter. The potential depth of the truncated sphere became half the limit when the opening diameter increased to the sphere diameter. These results suggest that the carbon cavity with cylindrical or spherical shape can increase the adsorption energy to nearly 150 meV if they have appropriate dimensions, and they will serve as the adsorption sites of the hydrogen storage materials working under mild conditions.

The optimum diameters of the cylinder and the sphere are close to the diameters of the narrowest carbon nanotube (~ 7 Å) and of C_{60} (7.12 Å), respectively. Carbon nanotubes are sonicated with acid to make the openings [22]. The opening on a C_{60} molecule can be made by a chemical process [23], and the encapsulation of a hydrogen molecule by the opening has been clearly demonstrated [24]. Therefore, in this paper, we investigate the hydrogen adsorption by a truncated carbon sphere under finite temperatures and pressures based on the Langmuir isotherm derived from the adsorption potential curve. In Sect. 2, we derive the adsorption potential curve using the Lennard–Jones potential function regarding the sphere surface as a continuum with a uniform density. In Sect. 3, we draw the Langmuir isotherm based on the adsorption eigenvalues calculated by the Wentzel–Kramers–Brillouin (WKB) approximation and give a crude estimation of the storage density of the material consisting of truncated carbon spheres based on the crystal structure of C_{60} . The

descriptions of the symbols used in this paper are summarized in the “Appendix”.

2 The potential energy curve for the adsorption of a hydrogen molecule by a hollow sphere consisting of carbon atoms

We derive the adsorption potential function of a hydrogen molecule bound in a truncated carbon sphere following the theory used in our previous paper [21]. We adopt the Lennard–Jones function for the pair interaction between a carbon atom and a hydrogen molecule separated by distance r . This is given by

$$V_{\text{LJ}}(r) = 4\epsilon_{\text{C-H}_2} \left[\left(\frac{\sigma_{\text{C-H}_2}}{r} \right)^{12} - \left(\frac{\sigma_{\text{C-H}_2}}{r} \right)^6 \right], \quad (1)$$

where $\epsilon_{\text{C-H}_2}$ and $\sigma_{\text{C-H}_2}$ denote the potential depth and the distance at which V_{LJ} crosses zero, respectively. This function has been used widely for a long time despite its obvious defects because it facilitates the analytical calculations [25].

Assuming the carbon atoms are continuously distributed on the sheet with a uniform density ρ_s , the adsorption energy can be obtained by integrating V_{LJ} over the sheet,

$$W = \rho_s \int_{\sigma} V_{\text{LJ}}(r) d\sigma, \quad (2)$$

where $d\sigma$ denotes the surface element of the sheet. In the case of a single graphene sheet with an infinite size, the adsorption energy of a hydrogen molecule located at the distance d above the sheet is calculated as [26]

$$W_{\text{sg}}(d) = \frac{D_{\text{sg}}}{3} \left[2 \left(\frac{d_{\text{sg}}}{d} \right)^{10} - 5 \left(\frac{d_{\text{sg}}}{d} \right)^4 \right], \quad (3)$$

where D_{sg} and d_{sg} denote the potential depth and the optimum distance, respectively, giving the minimum energy $-D_{\text{sg}}$. They are given as

$$D_{\text{sg}} = \frac{6}{5} \pi \rho_s \sigma_{\text{C-H}_2}^2 \epsilon_{\text{C-H}_2}, \quad (4)$$

$$d_{\text{sg}} = \sigma_{\text{C-H}_2}. \quad (5)$$

The values of $\epsilon_{\text{C-H}_2}$, $\sigma_{\text{C-H}_2}$, and ρ_s used in this paper are shown in Table 1. Values of $\epsilon_{\text{C-H}_2}$ and $\sigma_{\text{C-H}_2}$ were adopted from a scattering experiment of a hydrogen molecule from the (0001) graphite surface [3], and that of ρ_s was made to be identical to the surface density of the carbon layer of graphite.

The reliability of the whole methodology employed in our study depends on the degree of the accuracy of Eq. (2) obtained by integrating the Lennard–Jones potential over

Table 1 The values of the parameters used in the hydrogen adsorption potential

ρ_s (\AA^{-2})	$\epsilon_{\text{C-H}_2}$ (meV)	$\sigma_{\text{C-H}_2}$ (\AA)	D_{sg} (meV)	d_{sg} (\AA)	D (meV)	d_e (\AA)
0.382	3.89	2.89	46.8	2.89	203	3.37

ρ_s , the surface density of the nanocarbon; $\epsilon_{\text{C-H}_2}$, the depth of the Lennard–Jones potential between C and H₂; $\sigma_{\text{C-H}_2}$, the distance parameter of the potential; D_{sg} , the potential depth of the H₂ adsorption by an infinite single carbon sheet; d_{sg} , the distance from the sheet giving the potential minimum; D , the potential depth of the H₂ adsorption by a closed carbon sphere; d_e , the radius of the sphere giving the potential minimum

the carbon surface. The adopted values of the Lennard–Jones parameters ($\epsilon_{\text{C-H}_2}$ and $\sigma_{\text{C-H}_2}$) were determined by using the potential function derived from Eq. (3) (hence from Eq. 2) by summing up the attractive parts over the graphite layers and these parameters succeeded to reproduce the energy eigenvalues of the hydrogen adsorption on the graphite surface measured by the experiment [3]. These values yield $D_{\text{sg}} = 46.8$ meV and $d_{\text{sg}} = 2.89$ Å, which are close to those of the hydrogen adsorption on aromatic hydrocarbon molecules as calculated by the quantum chemical methods [13, 27]. The adoption of these parameter values is consistent with the use of Eq. (2). We suppose the use of Eq. (2) with those adopted parameters leads quantitatively credible results.

We examined the binding energy of a hydrogen molecule adsorbed in a truncated hollow sphere consisting of carbon atoms. In Fig. 1, we show the geometry of the truncated sphere with radius d and opening radius a . The origin of the system is located at the center of the sphere and the z -axis is drawn through the center of the opening. The axis crosses the opening at $z = d \cos \theta_a$, where θ_a represents the azimuthal angle of the opening edge ($\theta_a = \sin^{-1} a/d$). Adding a hydrogen molecule at a position along the z -axis and integrating Eq. (2) with respect to the azimuthal angle of the carbon surface θ from θ_a to π with

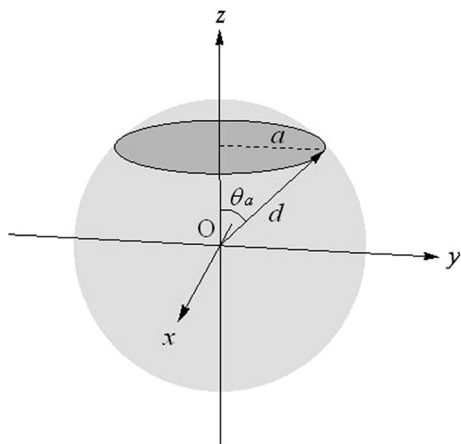


Fig. 1 The geometry of the truncated carbon sphere: d , the radius of the sphere; a , the radius of the opening; θ_a , the azimuthal angle of the opening edge. The H₂ molecule enters the sphere along the z -axis passing through the center of the opening

substitutions $r = \sqrt{d^2 + z^2 - 2dz \cos \theta}$ and $d\sigma = 2\pi d^2 \sin \theta d\theta$, we obtain the adsorption energy in the form as

$$W(z, d, a) = \frac{D}{3} \left\{ \frac{1}{10(z/d)} \left[\frac{1}{[1 - 2(z/d) \cos \theta_a + (z/d)^2]^5} - \frac{1}{[1 + (z/d)]^{10}} \right] \left(\frac{d_e}{d}\right)^{10} - \frac{5}{8(z/d)} \left[\frac{1}{[1 - 2(z/d) \cos \theta_a + (z/d)^2]^2} - \frac{1}{[1 + (z/d)]^4} \right] \left(\frac{d_e}{d}\right)^4 \right\}, \tag{6}$$

where D and d_e denote the potential depth and the optimum sphere radius, respectively, giving the minimum energy $-D$ at $z = 0$ when $a = 0$. They are given by

$$D = 8 \left(\frac{2}{5}\right)^{2/3} D_{\text{sg}}, \tag{7}$$

$$d_e = \left(\frac{5}{2}\right)^{1/6} d_{\text{sg}}. \tag{8}$$

The D is about 4.4 times as large as D_{sg} , and the d_e is about 1.2 times as large as d_{sg} . The values of D and d_e are 203 meV and 3.37 Å, respectively.

The form of Eq. (6) was derived without any approximation, and it holds for any position along the z -axis. In Eq. (6), the term proportional to $(d_e/d)^{10}$ represents the repulsive component and the term proportional to $(d_e/d)^4$ represents the attractive component of the potential. Both components include the factor having the form of $(z/d)^{-1} \{ [1 - 2(z/d) \cos \theta_a + (z/d)^2]^{-n} - [1 + (z/d)]^{-2n} \}$. In the case, when we can divide the carbon surface into the upper and lower parts at $\theta = \cos^{-1} z/2d$ where r becomes equal to d , the first term of this factor arises from the integration of the upper part and the second term arises from that of the lower part. They increase or decrease the potential components when the hydrogen molecule approaches or leaves these parts by moving along the z -axis. The first term depends on the size of the opening through the $\cos \theta_a$ term.

In the case of $d = d_e$, the adsorption energy of the truncated sphere at $z = 0$ is given by

$$W(0, d_e, a) = -\cos^2(\theta_a/2)D. \quad (9)$$

This formula gives $-0.93D$, $-0.75D$, and $-0.50D$ when $a = 0.50d_e$ ($\theta_a = \pi/6$), $0.87d_e$ ($\pi/3$), and d_e ($\pi/2$), respectively. In Fig. 2, we show the adsorption potential energy curve of the sphere with radius d_e upon changing a from zero to d_e . The curve becomes shallow with the increase of a . The deepest minimum of each curve is found near the origin, and its depth is close to that given by Eq. (9). The maximum, located near the opening at $z = d \cos \theta_a$, decreases as a increases. These maxima show negative values when a exceeds $0.74d_e$ ($\theta_a = \pi/4$) and are not observed when a approaches $0.87d_e$ ($\theta_a = \pi/3$). At $a = 0.87d_e$, the curve shows a smooth decrease until the incoming molecule reaches the minimum and a steep increase as the molecule approaches the opposite side of the opening. The minimum of this curve is -154 meV.

3 The Langmuir isotherm of hydrogen adsorption by the truncated sphere

We have shown that the carbon sphere with a radius of d_e truncated at $\theta_a = \pi/3$ has thermodynamic and kinetic advantages for hydrogen storage because of the deep adsorption potential and lack of energy barrier. We then examined the hydrogen adsorption by this sphere under finite temperatures and pressures based on the Langmuir isotherm, which we derived by using the statistical mechanics method. We need the eigenvalues of the adsorption potential curve to obtain the partition function of the adsorbed molecule. In Table 2, the eigenvalues calculated by the WKB method are shown with those of the hydrogen adsorption on the (0001) graphite surface obtained by

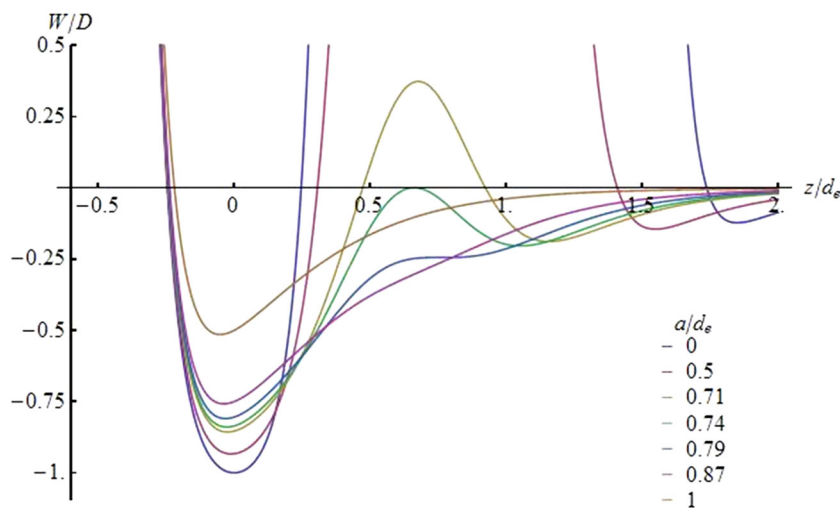
Table 2 The eigenvalues of the potential energy curve of the H_2 adsorption by the truncated carbon sphere and those by the (0001) graphite surface

n	ϵ_n (meV)	
	Truncated sphere	Graphite surface
0	-143.6	-41.6
1	-124.3	-26.4
2	-107.0	-15.3
3	-91.6	-8.0
4	-78.1	-3.6
5	-66.5	-1.5
6	-56.5	
7	-47.4	
8	-38.9	
9	-30.8	
10	-23.4	
11	-16.7	
12	-10.9	
13	-6.2	
14	-2.8	
15	-0.8	

The radius of the sphere and that of the opening are d_e and $\sqrt{3}/2d_e$, respectively. The eigenvalues of the sphere were calculated by the WKB method, and those of the graphite surface were obtained by experiment [3]

experiment [3]. The number of bound states used to evaluate the partition function is 16 for the sphere and 6 for the graphite surface. The lowest eigenvalue of the sphere is -144 meV, which is about three times lower than that of the graphite surface. In Fig. 3, the levels of the bound states are shown with the potential curve. The bottom of the curve (-154 meV) is located at $z = -0.13$ Å. The farthest turning point of the hydrogen molecule bound in the sphere is about $2d_e$.

Fig. 2 The potential energy curve with respect to the position of the H_2 molecule adsorbed by the truncated carbon sphere with a radius of d_e ($=3.37$ Å). The curve was plotted by changing the opening radius a from 0 to d_e . The deepest minimum $-D$ ($= -203$ meV) was obtained at $z = 0$ when $a = 0$



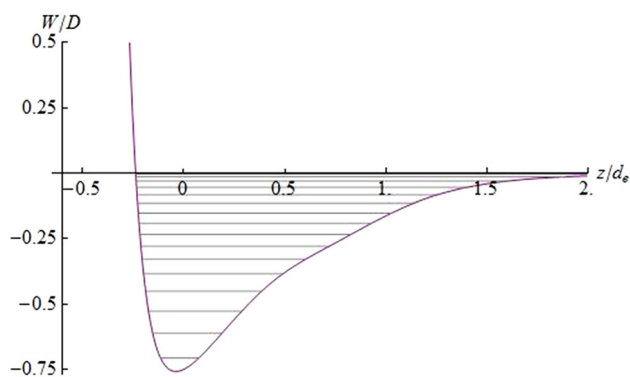


Fig. 3 The levels of the eigenvalues for the adsorption potential curve of the H₂ molecule bound in the truncated carbon sphere with the radius of d_e ($=3.37$ Å) and the opening radius of $a = \sqrt{3}/2d_e$ ($=2.92$ Å). The eigenvalues were calculated by the WKB method

We propose a hydrogen adsorption substrate consisting of truncated spheres with each sphere adsorbing up to one hydrogen molecule. The occupancy of the sphere at pressure p and temperature T is given by the Langmuir isotherm,

$$\theta(p, T) = \frac{p}{p + p_0(T)}, \tag{10}$$

where $p_0(T)$ denotes the pressure giving a half occupancy of the site at the given temperature and its reciprocal gives the equilibrium constant for the adsorption. This is given by [28]

$$p_0(T) = \frac{z_{\text{gas}}(T)}{z_{\text{ads}}(T)} k_B T, \tag{11}$$

where $z_{\text{gas}}(T)$ and $z_{\text{ads}}(T)$ denote the molecular partition function of the hydrogen gas per unit volume and that of the adsorbed molecule in the sphere, respectively. We regard the hydrogen molecule as both a point particle with mass m in the gas phase and one moving along the one-dimensional potential curve in the bound state. The partition functions are given by

$$z_{\text{gas}}(T) = \left(\frac{2\pi m k_B T}{h^2} \right)^{\frac{3}{2}} \tag{12}$$

for the gas molecule, and

$$z_{\text{ads}}(T) = \sum_n e^{-\epsilon_n/k_B T} \tag{13}$$

for the adsorbed molecule, where ϵ_n denotes the n th eigenvalue of the potential.

Table 3 presents the value of $p_0(T)$ of the truncated sphere and that of the graphite surface for temperatures between 60 and 300 K. The $p_0(T)$ of the truncated sphere is 212 bar at 300 K and becomes lower than 52 bar at temperatures below 250 K. Conversely, $p_0(T)$ of the graphite

Table 3 The half-occupancy pressure of the Langmuir isotherm at the temperature T for the truncated carbon sphere and the (0001) graphite surface

T (K)	$p_0(T)$ (bar)	
	Truncated sphere	Graphite surface
60	2×10^{-9}	6×10^{-1}
77	1×10^{-6}	6
100	4×10^{-4}	47
150	2×10^{-1}	508
200	7	1896
250	52	4574
300	212	8798

The radius of the sphere and that of the opening are d_e and $\sqrt{3}/2d_e$, respectively

surface shows larger values than those of the sphere at the same temperatures. The $p_0(T)$ decreases to 47 bar when the temperature is lowered to 100 K.

Figure 4 shows the isotherms at these temperatures for the truncated sphere and the graphite surface. The dashed lines in the figure are the contributions from the lowest eigenvalues. The isotherm of the truncated sphere at 250 K shows that the occupancy exceeds 0.8 when the pressure exceeds 208 bar. At 200 K, the occupancy reaches 0.8 at 28 bar. At 150 K, the occupancy approaches 1 under lower pressures, and almost all the molecules are bound in the lowest state. The graphite surface requires lower temperatures to achieve a large occupancy under low pressures compared with the truncated sphere. The occupancy exceeds 0.8 under pressures over 188 bar at 100 K and 24 bar at 77 K. The occupancy approaches 1 under lower pressures when the temperature is lowered to 60 K.

We estimated the storage density of the substrate by assuming that the substrate forms an fcc lattice which is identical to that of C₆₀. The lattice constant of a C₆₀ crystal is 14.15 Å, and the radius of C₆₀ sphere is 3.56 Å [29]. The unit cell of the fcc lattice has a net total of four lattice points and four octahedral and eight tetrahedral voids which use the lattice points as their vertexes. Therefore, we have four octahedral adsorption sites and eight tetrahedral sites between the spheres in addition to the four sites in the spheres. The distance from the center of the octahedral site to the sphere surface (opening) is 3.52 (5.30) Å and that from the center of the tetrahedral site to the sphere surface (opening) is 2.61 (4.39) Å. These sizes allow each site to accept one hydrogen molecule. The volume of the cell removing the truncated spheres becomes more than ten times as large as that of the sphere, so that each site has room to accept about one hydrogen molecule on average. Therefore, we consider that the unit cell has up to 16 adsorption sites, which gives a maximum storage density of

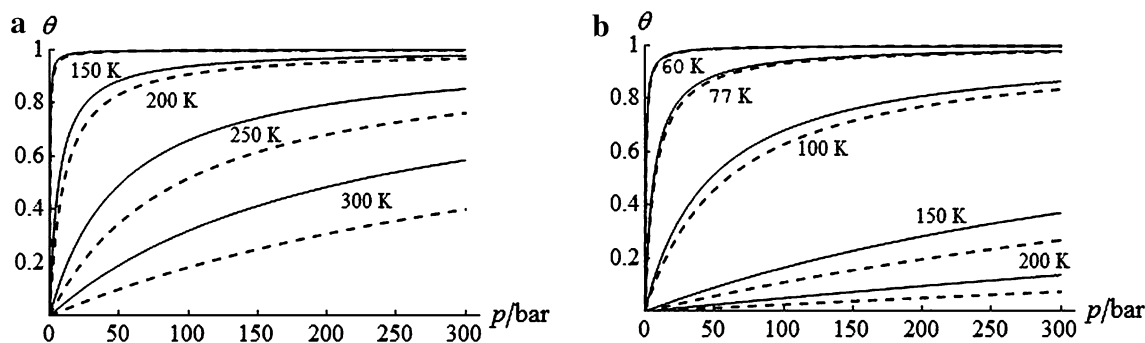


Fig. 4 Langmuir isotherms of the H_2 adsorption by carbon materials: **a** the truncated carbon sphere with a radius of $d_c (=3.37 \text{ \AA})$ and an opening radius of $a = \sqrt{3}/2d_c (=2.92 \text{ \AA})$, **b** the (0001) graphite surface. The *dashed lines* are the contributions from the lowest eigenvalues

18.9 g/L to the substrate. The intersphere sites possibly show large adsorption energies because the pore size is close to the optimum value ($\sim 7 \text{ \AA}$). For simplification in the analysis, we assume that the all adsorption sites have the same value of $p_0(T)$.

The number of hydrogen molecules per unit volume of the substrate and that of the gas are given, respectively, by

$$\overline{N}_{\text{H}_2}^{\text{ads}}(p, T) = \overline{N}_{\text{site}}\theta(p, T), \quad (14)$$

$$\overline{N}_{\text{H}_2}^{\text{gas}}(p, T) = \frac{p}{k_{\text{B}}T}, \quad (15)$$

where $\overline{N}_{\text{site}}$ denotes the number of the adsorption sites in the substrate per unit volume. The gradient of $\overline{N}_{\text{H}_2}^{\text{ads}}(p, T)$ with respect to p gives $\overline{N}_{\text{site}}/p_0(T)$ at $p = 0$. Therefore, for $\overline{N}_{\text{H}_2}^{\text{ads}}(p, T)$ to be larger than $\overline{N}_{\text{H}_2}^{\text{gas}}(p, T)$ under a constant temperature, the $\overline{N}_{\text{site}}$ must satisfy the condition,

$$\overline{N}_{\text{site}} > \frac{p_0(T)}{k_{\text{B}}T}. \quad (16)$$

This condition gives the lower limit of $\overline{N}_{\text{site}}$,

$$\overline{N}_0(T) = \frac{p_0(T)}{k_{\text{B}}T}. \quad (17)$$

The range of pressures where $\overline{N}_{\text{H}_2}^{\text{ads}}(p, T)$ exceeds $\overline{N}_{\text{H}_2}^{\text{gas}}(p, T)$ under a constant temperature is given by

$$0 < p < [\overline{N}_{\text{site}} - \overline{N}_0(T)]k_{\text{B}}T. \quad (18)$$

At the maximum pressure,

$$p_{\text{max}}(T) = [\overline{N}_{\text{site}} - \overline{N}_0(T)]k_{\text{B}}T, \quad (19)$$

$\overline{N}_{\text{H}_2}^{\text{ads}}(p, T)$ coincides with $\overline{N}_{\text{H}_2}^{\text{gas}}(p, T)$ and becomes

$$\overline{N}_{\text{H}_2}^{\text{ads}}(p_{\text{max}}, T) = \overline{N}_{\text{site}} - \overline{N}_0(T) \quad (20)$$

This equation indicates that $\overline{N}_0(T)$ refers to the density of vacant sites at p_{max} .

Using Eq. (11), we can rewrite Eq. (17) as

$$\overline{N}_0(T) = \frac{z_{\text{gas}}(T)}{z_{\text{ads}}(T)}. \quad (21)$$

This equation determines the lowest eigenvalue of the potential (ϵ_0) necessary to make $\overline{N}_{\text{H}_2}^{\text{ads}}(p, T)$ larger than $\overline{N}_{\text{H}_2}^{\text{gas}}(p, T)$ if the eigenvalues other than ϵ_0 can be ignored. This is given by

$$\epsilon_0 = -k_{\text{B}}T \ln \frac{z_{\text{gas}}(T)}{\overline{N}_0(T)}. \quad (22)$$

The right-hand side of this equation represents the chemical potential of the gas molecule with the density of $\overline{N}_0(T)$. When $\overline{N}_{\text{site}}$ is equivalent to the number of hydrogen molecules corresponding to the target density of 40 g/L (i.e., 34 molecules in the unit cell under consideration) and the storage is performed at 300 K, ϵ_0 is required to be deeper than -140 meV because $\overline{N}_0(T)$ must be smaller than $\overline{N}_{\text{site}}$ for the storage density to exceed the gas density. The ϵ_0 needs -160 meV to occupy 50 % of $\overline{N}_{\text{site}}$ at $p_{\text{max}}(T) = 250 \text{ bar}$, and it needs -200 meV to occupy 90 % of $\overline{N}_{\text{site}}$ at $p_{\text{max}}(T) = 450 \text{ bar}$. To strengthen hydrogen binding, adding Li or Be atoms into carbon cavities is one of the methods [27].

We estimate the values of $\overline{N}_0(T)$ and $\overline{N}_{\text{H}_2}^{\text{ads}}(p_{\text{max}}, T)$ of the substrate by assuming that the adsorption sites in the substrate have the same $p_0(T)$ as the truncated sphere with the optimum radius (3.37 \AA). Taking the volume of the unit cell as unity, we show these values with volumetric and gravimetric densities in Table 4. At 300 K, $\overline{N}_0(T)$ becomes 14.5 and this value restricts $\overline{N}_{\text{site}}$ to 16. These values yield a $\overline{N}_{\text{H}_2}^{\text{ads}}(p_{\text{max}}, T)$ of 1.5 at $p_{\text{max}}(T) = 21 \text{ bar}$, where the occupancy is 0.1. The volumetric and gravimetric densities are 1.7 g/L and 0.1 wt%, respectively. At 250 K, $\overline{N}_0(T)$ becomes 4.2 and this restricts $\overline{N}_{\text{site}}$ to 8–16. The value of $\overline{N}_{\text{H}_2}^{\text{ads}}(p_{\text{max}}, T)$ increases from 3.8 (at 46 bar) to 11.8 (at 143 bar) with the increase of $\overline{N}_{\text{site}}$ from 8 to 16. Along with

Table 4 The extent of hydrogen storage at the temperature T in the fcc unit cell of the substrate consisting of the truncated spheres

T (K)	$\overline{N}_{\text{site}}$	$\overline{N}_0(T)$	$p_{\text{max}}(T)$ (bar)	$\overline{N}_{\text{H}_2}^{\text{ads}}(p_{\text{max}}, T)$	d_v (g L ⁻¹)	d_g (wt%)
150	4	0.0	29	4.0	4.7	0.4
	8		58	8.0	9.4	0.7
	12		87	12.0	14.1	1.1
	16		117	16.0	18.9	1.5
200	4	0.7	32	3.3	3.9	0.3
	8		71	7.3	8.7	0.7
	12		110	11.3	13.4	1.1
	16		149	15.3	18.1	1.4
250	8	4.2	46	3.8	4.4	0.4
	12		95	7.8	9.2	0.7
	16		143	11.8	13.9	1.1
300	16	14.5	21	1.5	1.7	0.1

$\overline{N}_{\text{site}}$, the number of the adsorption sites in the unit cell; $\overline{N}_0(T)$, the lower limit of the $\overline{N}_{\text{site}}$; $p_{\text{max}}(T)$, the pressure at which the substrate has the same density as the gas; $\overline{N}_{\text{H}_2}^{\text{ads}}(p_{\text{max}}, T)$, the number of H₂ molecules in the unit cell at $p_{\text{max}}(T)$; d_v , the volumetric density; d_g , the gravimetric density. The $\overline{N}_{\text{H}_2}^{\text{ads}}(p_{\text{max}}, T)$ is given by $\overline{N}_{\text{site}} - \overline{N}_0(T)$

this change, the occupancy increases from 0.46 to 0.73. The volumetric and gravimetric densities were 4.4–13.9 g/L and 0.4–1.1 wt%, respectively. Below 200 K, $\overline{N}_0(T)$ becomes lower than 1 and all sites are available. At 200 K, $\overline{N}_{\text{H}_2}^{\text{ads}}(p_{\text{max}}, T)$ increases from 3.3 (at 32 bar) to 15.3 (at 149 bar) with the increase of $\overline{N}_{\text{site}}$ from 4 to 16. The occupancy changes from 0.83 to 0.96. The volumetric and gravimetric densities were 3.9–18.1 g/L and 0.3–1.4 wt%, respectively. At 150 K, all sites are occupied at $p_{\text{max}}(T)$. The $\overline{N}_{\text{H}_2}^{\text{ads}}(p_{\text{max}}, T)$ reaches the upper limit of 16.0 at 117 bar. This yields 18.9 g/L for the volumetric and 1.5 wt% for the gravimetric densities.

4 Conclusions

We showed that the truncated carbon sphere with a radius of 3.37 Å adsorbed a hydrogen molecule with large adsorption energy (~ 150 meV) and no energy barrier when the opening radius was 2.92 Å. The Langmuir isotherm of this sphere showed that the occupancy exceeded 0.5 at lower pressures than 50 bar at temperatures below 250 K. This indicates that the sphere can store hydrogen molecules under mild conditions. We suggest a substrate consisting of the truncated spheres which form an fcc lattice identical to that of the C₆₀ crystal. Assuming that the substrate had up to 16 adsorption sites in the unit cell, we obtained the maximum storage density of 18.9 g/L at 117 bar and 150 K, where all sites were occupied.

We showed that $\overline{N}_{\text{site}}$ and $\overline{N}_0(T)$ controlled the storage density. The former is a structural quantity depending on the shape and size of the adsorption site, and the latter is an

energetics quantity determined by the eigenvalues of the adsorption potential inherent to the adsorption site. To achieve a large amount of storage, the substrate should increase the density of the adsorption sites by optimizing their shape and size to give them large adsorption energies. We propose hydrogen adsorption in the intrasphere and intersphere sites. However, the adsorption sites should take polyhedral structures that fill the unit cell to maximize the number of adsorption sites in the cell which distributes the large adsorption energy equally to each site. We need 34 adsorption sites in the unit cell to achieve the target density of 40 g/L. Creating these sites in carbon materials is likely to be impossible judging from the optimum size of the carbon pore. To approach the target volume density with $\overline{N}_{\text{site}} \approx 16$, some or all sites must adsorb more than two molecules. This requires greater adsorption potential energies.

Conflict of interest The authors declare that they have no conflict of interest.

Appendix: List of symbols

Symbols	Description
$\epsilon_{\text{C-H}_2}$	Lennard–Jones potential depth between C and H ₂
ϵ_n	The n th eigenvalue of the potential energy curve for the H ₂ adsorption
θ	Azimuthal angle of the surface of the truncated carbon sphere
θ_a	Azimuthal angle of the opening edge on the truncated carbon sphere

continued

Symbols	Description
$\theta(p, T)$	Occupancy of the H ₂ adsorption site given by the Langmuir isotherm
ρ_s	Surface density of the carbon sheet
σ_{C-H_2}	Lennard–Jones distance parameter between C and H ₂
a	Opening radius of the truncated carbon sphere
d	Radius of the truncated carbon sphere or the distance between H ₂ and an infinite single carbon sheet
d_e	Equilibrium radius of the closed carbon sphere for the H ₂ adsorption
d_g	Gravimetric H ₂ density of the substrate
$d\sigma$	Surface element of the carbon surface
d_{sg}	Equilibrium distance between H ₂ and an infinite single carbon sheet
d_v	Volumetric H ₂ density of the substrate
D	Potential depth of the H ₂ adsorption by the closed carbon sphere
$\overline{N}_0(T)$	Lower limit of the number density of the H ₂ adsorption sites
\overline{N}_{site}	Number density of the H ₂ adsorption sites
$\overline{N}_{H_2}^{ads}(p, T)$	Number density of adsorbed H ₂ molecules in the substrate
$\overline{N}_{H_2}^{gas}(p, T)$	Number density of gaseous H ₂ molecules
$p_0(T)$	Half-occupancy pressure of the Langmuir isotherm for the H ₂ adsorption
$p_{max}(T)$	Pressure at which the substrate has the same H ₂ density as the gas
r	Distance between C and H ₂
z	Position of the H ₂ molecule adsorbed by the truncated carbon sphere
$z_{ads}(T)$	Molecular partition function of the adsorbed H ₂ molecule
$z_{gas}(T)$	Molecular partition function of the gaseous H ₂ molecule per unit volume
$V_{LJ}(r)$	Lennard–Jones potential
W	Integral form of the H ₂ adsorption energy
$W_{sg}(d)$	H ₂ adsorption energy by an infinite single carbon sheet
$W(z, d, a)$	H ₂ adsorption energy by the truncated carbon sphere

References

1. Fuel Cell Technologies Office Multi-Year Research, Development, and Demonstration Plan, Section 3.3 Hydrogen Storage,

- 2012 <http://energy.gov/sites/prod/files/2014/03/f12/storage.pdf>. Accessed 12 Dec 2014
- S.K. Bhatia, A.L. Myers, Langmuir **22**, 1688 (2006)
 - L. Mattera, F. Rosatelli, C. Salvo, F. Tommasini, U. Valbusa, G. Vidali, Surf. Sci. **93**, 515 (1980)
 - P. Bénard, R. Chahine, Langmuir **17**, 1950 (2001)
 - U. Eberle, M. Felderhoff, F. Schüth, Angew. Chem. Int. Ed. **48**, 6608 (2009)
 - S. Patchkovskii, J.S. Tse, S.N. Yurchenko, L. Zhchikov, T. Heine, G. Seifert, Proc. Natl. Acad. Sci. USA **102**, 10439 (2005)
 - H. Cheng, A.C. Cooper, G.P. Pez, M.K. Kostov, P. Piotrowski, S.J. Stuart, J. Phys. Chem. B **109**, 3780 (2005)
 - B. Kuchta, L. Fírllej, P. Pfeifer, C. Wexler, Carbon **48**, 223 (2010)
 - K.M. Thomas, Catal. Today **120**, 389 (2007)
 - W.J. Fan, R.Q. Zhang, B.K. Teo, B. Aradi, Th. Frauenheim, Appl. Phys. Lett. **95**, 013116 (2009)
 - G. Mpourmpakis, G.E. Froudakis, G.P. Lithoxoos, J. Samios, J. Chem. Phys. **126**, 144704 (2007)
 - I. Cabria, M.J. Lopez, J.A. Alonso, Carbon **45**, 2649 (2007)
 - J.A. Alonso, I. Cabria, M.J. Lopez, J. Mex. Chem. Soc. **56**, 261 (2012)
 - Q. Wang, J.K. Johnson, J. Chem. Phys. **110**, 577 (1999)
 - P. Kowalczyk, P.A. Gauden, A.P. Terzyk, S.K. Bhatia, Langmuir **23**, 3666 (2007)
 - W.-Q. Deng, X. Xu, W.A. Goddard, Phys. Rev. Lett. **92**, 166103-1 (2004)
 - M.T. Knippenberg, S.J. Stuart, A.C. Cooper, G.P. Pez, H. Cheng, J. Phys. Chem. B **110**, 22957 (2006)
 - C.-I. Weng, S.-P. Ju, K.-C. Fang, F.-P. Chang, Comput. Mater. Sci. **40**, 300 (2007)
 - S.S. Han, H.S. Kim, K.S. Han, J.Y. Lee, H.M. Lee, J.K. Kang, S.I. Woo, A.C.T. van Duin, W.A. Goddard, Appl. Phys. Lett. **87**, 213113 (2005)
 - T. Yamabe, M. Fujii, S. Mori, H. Kinoshita, S. Yata, Synth. Met. **145**, 31 (2004)
 - S. Ishikawa, T. Yamabe, Appl. Phys. A **114**, 1339 (2014)
 - M. Hirscher, M. Becher, M. Haluska, U. Dettlaff-Weglikowska, A. Quintet, G.S. Duesberg, Y.-M. Choi, P. Downes, M. Hulman, S. Roth, I. Stepanek, P. Bernier, Appl. Phys. A **72**, 129 (2001)
 - Y. Murata, M. Murata, K. Komatsu, J. Org. Chem. **66**, 8187 (2001)
 - Y. Murata, M. Murata, K. Komatsu, J. Am. Chem. Soc. **125**, 7152 (2003)
 - A.J. Stone, *The Theory of Intermolecular Forces*, 1st edn. (Clarendon Press, Oxford, 2002)
 - W.A. Steele, *The Interaction of Gases with Solid Surfaces*, 1st edn. (Pergamon Press, New York, 1974)
 - S. Ishikawa, T. Yamabe, Appl. Phys. A **99**, 29 (2010)
 - R. Kubo, *Statistical Mechanics*, 2nd edn. (Elsevier, Amsterdam, 2004)
 - W.P. David, R.M. Ibberson, J.C. Matthewman, K. Prassides, T.J.S. Dennis, J.P. Hare, H.W. Kroto, R. Taylor, D.R.M. Wlaton, Nature **353**, 147 (1991)